

See discussions, stats, and author profiles for this publication at: <https://www.researchgate.net/publication/11756855>

# Conformational Dynamics of the Transcriptional Regulator CooA Protein Studied by Subpicosecond Mid-Infrared Vibrational Spectroscopy

ARTICLE in JOURNAL OF THE AMERICAN CHEMICAL SOCIETY · NOVEMBER 2001

Impact Factor: 12.11 · DOI: 10.1021/ja011023w · Source: PubMed

---

CITATIONS

26

---

READS

22

7 AUTHORS, INCLUDING:



Hiroshi Nakajima

Nagoya University

72 PUBLICATIONS 1,407 CITATIONS

SEE PROFILE



Shigeichi Kumazaki

Kyoto University

41 PUBLICATIONS 653 CITATIONS

SEE PROFILE



Keitaro Yoshihara

The Graduate University for Advanced Studies

302 PUBLICATIONS 7,910 CITATIONS

SEE PROFILE

# Conformational Dynamics of the Transcriptional Regulator CooA Protein Studied by Subpicosecond Mid-Infrared Vibrational Spectroscopy

Igor V. Rubtsov,<sup>\*,†</sup> Tieqiao Zhang, Hiroshi Nakajima, Shigetoshi Aono, Grigori I. Rubtsov,<sup>‡</sup> Shigeichi Kumazaki, and Keitaro Yoshihara\*

Contribution from the School of Materials Science, Japan Advanced Institute of Science and Technology, Tatsunokuchi, Ishikawa 923-1292, Japan

Received April 23, 2001. Revised Manuscript Received July 10, 2001

**Abstract:** CooA, which is a transcriptional regulator heme protein allosterically triggered by CO, is studied by femtosecond visible-pump mid-IR-probe spectroscopy. Transient bleaching upon excitation of the heme in the Soret band is detected at  $\sim 1979\text{ cm}^{-1}$ , which is the absorption region of the CO bound to the heme. The bleach signal shows a nonexponential decay with time constants of 56 and 290 ps, caused by the rebinding of the CO to the heme. About 98% of dissociated CO recombines geminately. The geminate recombination rate in CooA is significantly faster than those in myoglobin and hemoglobin. The angle of the bound CO with respect to the porphyrin plane is calculated to be about  $78^\circ$  on the basis of the anisotropy measurements. A shift of the bleached mid-IR spectrum of the bound CO is detected and has a characteristic time of 160 ps. It is suggested that the spectral shift is caused by a difference in the frequency of the bound CO in different protein conformations, particularly in an active conformation and in an intermediate one, which is on the way toward an inactive conformation. Thus, the biologically relevant conformation change in CooA was traced. Possible assignment of the observed conformation change is discussed.

## Introduction

Several heme proteins were recently found in which biological function is triggered by the binding of small molecules such as NO, O<sub>2</sub>, and CO. Guanylyl cyclase is an NO sensor,<sup>1,2</sup> while FixL, HemAT, and Dos proteins are sensors for O<sub>2</sub>,<sup>3–5</sup> and CooA is a sensor for CO.<sup>6–10</sup> CooA is a homodimer of 24.6 kDa subunits containing a protoheme found in a photosynthetic bacterium, *Rhodospirillum rubrum*.<sup>6</sup> *R. rubrum* can grow with carbon monoxide as its sole energy source.<sup>10</sup> CooA is a CO sensor, which functions as a transcriptional activator. CO is a unique messenger to trigger DNA binding in CooA protein. The only other molecule found which is able to bind the heme of

the wild-type CooA is NO, though it does not induce CooA to bind its target DNA.<sup>11,12</sup> As the biological function of CooA is triggered by binding with CO, it is important to study the CO binding reaction and geometry of CO ligation. In this work, we study the CO–CooA binding and dissociation processes by means of time-resolved spectroscopy with a subpicosecond time resolution. Photoexcitation of the heme in the CO-bound CooA triggers CO dissociation.<sup>13,14</sup> If CO escapes from the heme pocket, recombination is a slow bimolecular reaction. Nanosecond flash photolysis has shown that nongeminate rebinding of CO from solution proceeds on a millisecond time scale with a rate constant of  $\sim 10\text{ (}\mu\text{M s)}^{-1}$ .<sup>13</sup> The electronic absorption and EPR spectra indicate that the CooA heme in its ferric (Fe<sup>III</sup>), ferrous (Fe<sup>II</sup>), and CO-bound states is low-spin and six-coordinate.<sup>8,9,13</sup> It was shown that Cys75 is the axial ligand in the ferric heme on the proximal side, but it switches to His77 in the ferrous form.<sup>9,15</sup> The X-ray structure of CooA showed that the second ligand of the ferrous heme without CO is an N-terminal group of Pro2 from the opposite subunit in the CooA homodimer.<sup>16</sup> Therefore, replacement of this ligand by CO is

<sup>†</sup> Present address: Department of Chemistry, University of Pennsylvania, Philadelphia, PA 19104-6323. E-mail: irubtsov@sas.upenn.edu.

<sup>‡</sup> Department of Physics, Lomonosov Moscow State University, Vorobyevy Gory, Moscow 119899, Russia.

(1) Ignaro, L. J.; Degnan, J. N.; Baricos, W. H.; Kadowitz, P. J.; Wolin, M. S. *Biochim. Biophys. Acta* **1982**, *718*, 49–59.

(2) Craven, P. A.; DeRubeis, F. R. *Biochim. Biophys. Acta* **1983**, *745*, 310–321.

(3) Gilles-Gonzalez, M. A.; Ditta, G. S.; Helinski, D. R. *Nature (London)* **1991**, *350*, 170–172.

(4) Hou, S.; Larsen, R. W.; Boudko, D.; Riley, C. W.; Karatan, E.; Zimmer, M.; Ordal, G. W.; Alam, M. *Nature (London)* **2000**, *403*, 540–544.

(5) Delgado-Nixon, V. M.; Gonzalez, G.; Gilles-Gonzalez, M. A. *Biochemistry* **2000**, *39*, 2685–2691.

(6) Shelper, D.; Kerby, R. L.; He, Y.-P.; Roberts, G. P. *J. Bacteriol.* **1995**, *171*, 2157–2163.

(7) Aono, S.; Nakajima, H.; Saito, K.; Okada, M. *Biochem. Biophys. Res. Commun.* **1996**, *228*, 752–756.

(8) Shelper, D.; Kerby, R. L.; He, Y.-P.; Roberts, G. P. *Proc. Natl. Acad. Sci. U.S.A.* **1997**, *94*, 11216–11220.

(9) Aono, S.; Ohkubo, K.; Matsuo, T.; Nakajima, H. *J. Biol. Chem.* **1998**, *273*, 25757–25764.

(10) Kerby, R. L.; Ludden, P. W.; Roberts, G. P. *J. Bacteriol.* **1995**, *177*, 2241–2244.

(11) Thorsteinsson, M. V.; Kerby, R. L.; Roberts, G. P. *Biochemistry* **2000**, *39*, 8284–8290.

(12) Reynolds, M. F.; Parks, R. B.; Burstyn, J. N.; Shelper, D.; Thorsteinsson, M. V.; Kerby, R. L.; Roberts, G. P.; Vogel, K. M.; Spiro, T. G. *Biochemistry* **2000**, *39*, 388–396.

(13) Uchida, T.; Ishikawa, H.; Takahashi, S.; Ishimori, K.; Morishima, I.; Ohkubo, K.; Nakajima, H.; Aono, S. *J. Biol. Chem.* **1998**, *273*, 19988–19992.

(14) Kumazaki, S.; Nakajima, H.; Sakaguchi, T.; Nakagawa, E.; Shino-hara, H.; Yoshihara, K.; Aono, S. *J. Biol. Chem.* **2000**, *275*, 38378–38383.

(15) Uchida, T.; Ishikawa, H.; Ishimori, K.; Morishima, I.; Nakajima, H.; Aono, S.; Mizutani, Y.; Kitagawa, T. *Biochemistry* **2000**, *39*, 12747–12752.

(16) Lanzilotta, W. N.; Schuller, D. J.; Thorsteinsson, M. V.; Kerby, R. L.; Roberts, G. P.; Poulos, T. L. *Nat. Struct. Biol.* **2000**, *7*, 876–880.

probably one of the key events that trigger the allosteric conformational change, which results in DNA binding. Contrary to this, CO dissociation causes a CooA conformational change from the functionally active structure to the inactive one. The CooA conformational change caused by CO photodissociation can be monitored by means of time-resolved spectroscopic methods. In this work, we focus on the geminate CO rebinding to the heme monitoring the IR absorption spectra of the bound CO.

The spectroscopic properties and dynamics of CooA were compared to other heme proteins, particularly hemoglobin (Hb) and myoglobin (Mb). These proteins were intensively studied by various spectroscopic methods combined with site-directed mutagenesis (for examples, see ref 17–38). It was shown spectroscopically that CO is bound to the heme of Mb/Hb along a direction tilted at an angle ( $\alpha$ ) of  $\sim 7$ – $10^\circ$  from the normal to the heme plane.<sup>24–28</sup> Although these results are in disagreement with earlier X-ray analysis, they have recently been supported by a new X-ray experiment with higher spatial resolution.<sup>29</sup> Upon electronic photoexcitation of the heme, CO dissociates with an essentially unit probability.<sup>18</sup> About 96% of the dissociated CO leaves the protein pocket in Mb, with only 4% recombining geminately.<sup>20</sup> In Hb, the percent of CO that recombines geminately depends on quaternary protein structure.<sup>16</sup> The geminate recombination time constant has been reported to be  $\sim 100$  ns for Hb in the R state<sup>19</sup> and about several microseconds for Mb<sup>20</sup> and Hb in the T state.<sup>19</sup> In some cases, however, recombination is much faster; the recombination of NO with Mb<sup>30</sup> is on the subnanosecond time scale. Two factors,

steric hindrance<sup>29,39</sup> and distal pocket polarity,<sup>40–42</sup> were considered to be important for the binding of small molecules to heme. On the other hand, variations in the stretching frequencies of the bound CO ( $\nu_{\text{C-O}}$  and  $\nu_{\text{Fe-CO}}$ ) in the myoglobins, including their mutants, were shown to be mostly determined by the polarity of the distal pocket and could not be explained by geometrical bond distortions.<sup>40–43</sup>

In this paper, we report the dynamics of CO dissociation, geminate rebinding of CooA, and conformational changes of the heme protein at a very early stage after CO dissociation by subpicosecond time-resolved mid-IR spectroscopy. The bleach spectrum of the bound CO stretching mode is found to evolve over time. Different frequencies of the bound CO observed are thought to arise from different protein conformations. The angle of the bound CO in CooA is determined to be  $\sim 78^\circ$  to the heme plane. Conformational changes around the heme take place with a time constant of  $\sim 100$  ps. The rate of CO recombination with heme is significantly faster than those for Mb and Hb.

## Experimental Section

**A. IR Spectrometer.** The UV–visible pump mid-IR probe spectrometer is based on a Ti:S laser system consisting of a generator, regenerative amplifier, and optical parametric amplifier (OPA) (Spectra Physics).<sup>44</sup> The OPA is pumped by a pulse train of 800 nm light with a subhundred femtosecond pulse duration at a 1 kHz repetition rate and power of 450 mW. This gives about 50–70  $\mu\text{J}$  total energy for the signal and idler pulses. The signal and idler pulses, separated by a dichroic mirror, passed through an optical delay line and recombined by a second dichroic mirror in a type I AgGaS<sub>2</sub> crystal of 2 mm thickness for difference frequency generation.<sup>45</sup> The bandwidth of the mid-IR pulses is about 150  $\text{cm}^{-1}$ . The mid-IR beam is divided into two parts, the probe and the reference, by a 50% Al mirror on a CaF<sub>2</sub> substrate. The probe beam is focused onto a sample cell by a 12 cm CaF<sub>2</sub> lens, yielding a spot size of  $\sim 120 \mu\text{m}$ . The second harmonic (SH) of the residual fundamental light after the OPA is used for an excitation pulse (pump pulse) in this experiment. The pump pulses are chopped at half of the repetition rate of the laser pulses and passed through a variable delay line, variable neutral-density filter, and half-wave plate. They are focused onto the sample cell by a 17 cm lens resulting in a spot size of 150  $\mu\text{m}$ . Finally, the probe and the vertically displaced reference beams are focused onto the entrance slit of a monochromator, in which a mirror is installed to separate two beams into two outputs. Two mercury cadmium telluride (MCT) detectors (Kolmar Technologies) with active sizes of  $2 \times 2 \text{ mm}^2$  and built-in amplifiers are attached to the monochromator. The instrument response function (fwhm) is estimated to be less than 250 fs by measuring the electronic response of a thin silicon plate. The instrument is controlled by a homemade program, which allows variable time steps in one scan.

The anisotropy measurements are made by rotating the polarization of the pump beam with the half-wave plate. About 10 scans with alternating polarization of the pump are performed to obtain anisotropy data. A baseline noise level of  $< 10^{-4}$  absorbance in an accumulation time of 2 s (thousand pulses for each case, with and without pump) was achieved.

**B. Sample Preparation.** Production and purification of the CooA protein were performed as recently described.<sup>7,9</sup> The final heme concentration of the CooA sample was  $\sim 1.5 \text{ mM}$ . Trisoboric acid buffer with a pH of 8.0 was used. Water was exchanged to D<sub>2</sub>O by a repeated

- (17) Li, X.-Y.; Spiro, T. G. *J. Am. Chem. Soc.* **1988**, *110*, 6024–6033.
- (18) Petrich, J. W.; Poyart, C.; Matrin, J. L. *Biochemistry* **1988**, *27*, 4049–4060.
- (19) Murray, L. P.; Hofrichter, J.; Henry, E. R.; Ikeda-Saito, M.; Kitagashi, K.; Yonetani, T.; Eaton, W. A. *Proc. Natl. Acad. Sci. U.S.A.* **1988**, *85*, 2151–2155.
- (20) Henry, E. R.; Sommer, J. H.; Hofrichter, J.; Eaton, W. A. *J. Mol. Biol.* **1983**, *166*, 443–451.
- (21) Anfinsen, P. A.; Han, C.; Hochstrasser, R. M. *Proc. Natl. Acad. Sci. U.S.A.* **1989**, *86*, 8387–8391.
- (22) Lian, T. B.; Locke, T.; Kitagawa, T.; Nagai, M.; Hochstrasser, R. M. *Biochemistry* **1993**, *32*, 5809–5814.
- (23) Lian, T.; Locke, B.; Kholodenko, Y.; Hochstrasser, R. M. *J. Phys. Chem.* **1994**, *98*, 11648–11656.
- (24) Locke, B.; Lian, T.; Hochstrasser, R. M. *Chem. Phys.* **1991**, *158*, 409–417.
- (25) Locke, B.; Lian, T.; Hochstrasser, R. M. *Chem. Phys.* **1995**, *190*, 155–156.
- (26) Lim, M.; Jackson, T. A.; Anfinrud, P. A. *Science* **1995**, *269*, 962–966.
- (27) Lim, M.; Jackson, T. A.; Anfinrud, P. A. *J. Phys. Chem.* **1996**, *100*, 12043–12051.
- (28) Ivanov, D.; Sage, J. T.; Keim, M.; Powell, J. R.; Asher, S. A.; Champion, P. M. *J. Am. Chem. Soc.* **1994**, *116*, 4139–4140.
- (29) Kachalova, G. S.; Popov, A. N.; Bartunik, H. D. *Science* **1999**, *284*, 473–476.
- (30) Shreve, A. P.; Franzen, S.; Simpson, M. C.; Dyer, R. B. *J. Phys. Chem. B* **1999**, *103*, 7969–7975.
- (31) Dlott, D. D.; Fayer, M. D.; Hill, J. R.; Rella, C. W.; Suslick, K. S.; Ziegler, C. J. *J. Am. Chem. Soc.* **1996**, *118*, 7853–7854.
- (32) Lim, M.; Jackson, T. A.; Anfinrud, P. A. *Nat. Struct. Biol.* **1997**, *4*, 209–214.
- (33) Yang, F.; Phillips, G. N., Jr. *J. Mol. Biol.* **1996**, *256*, 762–774.
- (34) Phillips, G. N., Jr.; Teodoro, M. L.; Li, T.; Smith, B.; Olson, J. S. *J. Phys. Chem. B* **1999**, *103*, 8817–8829.
- (35) Mizutani, Y.; Yamamoto, K.; Kitagawa, T. *Old and new views of protein folding*; Kuwajima, K., Arai, M., Eds.; Elsevier: New York, 1999; pp 85–94.
- (36) Hill, J. R.; Dlott, D. D.; Rella, C. W.; Peterson, K. A.; Decatur, S. M.; Boxer, S. G.; Fayer, M. D. *J. Phys. Chem.* **1996**, *100*, 12100–12107.
- (37) Walker, G. C.; Hochstrasser, R. M. *Laser Techniques in Chemistry*; Myers, A. B., Rizzo, T. R., Eds.; John Wiley & Sons: New York, 1995; Vol. XXIII.
- (38) Rella, C. W.; Kwok, A.; Rector, K.; Hill, J. R.; Schwettman, H. A.; Dlott, D. D.; Fayer, M. D. *Phys. Rev. Lett.* **1996**, *77*, 1648–1651.

- (39) Sleboznick, C.; Ibers, J. A. *J. Biol. Inorg. Chem.* **1997**, *2*, 521.
- (40) Grosh, A.; Bocian, D. F. *J. Phys. Chem.* **1996**, *100*, 6363–6367.
- (41) Kushkuley, B.; Stavrov, S. S. *Biophys. J.* **1997**, *72*, 899–912.
- (42) Spiro, T. G.; Kozlowski, P. M. *J. Am. Chem. Soc.* **1998**, *120*, 4524–4525.
- (43) Laberge, M.; Sharp, K. A.; Vanderkooi, J. M. *J. Phys. Chem. B* **1997**, *101*, 7364–7367.
- (44) Rubtsov, I. V.; Zhang, T.; Yoshihara, K. *Bunko Kenkyu* **2000**, *49*, 292–296.
- (45) Akhremichev, B.; Wang, C.; Walker, G. C. *Rev. Sci. Instrum.* **1996**, *67*, 3799–3805.

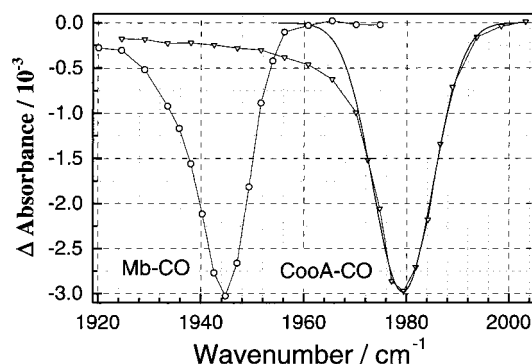


**Figure 1.** Transient absorption spectra of CooA-CO and Mb-CO measured at 1.4 ps time delay and for perpendicular ( $\perp$ ) polarizations of the pump with respect to the probe polarization. Spectral resolution is  $3.6 \text{ cm}^{-1}$ , and pump energy is 300 nJ/pulse. The Gaussian fit is shown at the full width at half-maximum of  $13.8 \pm 0.3 \text{ cm}^{-1}$ .

dilution/concentration procedure. The estimated amount of  $\text{H}_2\text{O}$  left was less than 5%. The CooA sample with the heme in ferric form was degassed and reduced by an excess amount of sodium dithionite. The CO-bound CooA was prepared by introducing gaseous CO into the reduced sample. The sample cell was filled in a glovebox under a nitrogen atmosphere.

**C. Experimental Conditions.** The sample cell was made of two 1 mm thick  $\text{CaF}_2$  windows and a spacer of 0.2 mm. The sample cell was kept constantly spinning to avoid heating and degradation. The spin rate was adjusted to ensure that a new location in the sample cell was excited for each pulse. The samples were kept at about  $+5^\circ\text{C}$  during the experiment by a flow of cooled nitrogen. The excitation power was reduced to  $\sim 0.3\text{--}0.4 \mu\text{J/pulse}$ , yielding an excitation of less than 20% of the hemes. The spectral resolution was  $3.6 \text{ cm}^{-1}$ . The integrity of the samples was frequently checked by measuring steady-state absorption spectra. Degradation of the sample after the experiments was less than 5%, as estimated from the main absorption peaks of the heme.

## Results

**A. CO Recombination.** The transient absorption spectrum of the CooA-CO sample in  $\text{D}_2\text{O}$  measured at a 1.4 ps time delay after photoexcitation of the heme is shown in Figure 1. The Mb-CO spectrum is also shown for comparison. The CooA spectrum shows a single peak with a long tail on the lower frequency side, which is in good agreement with the previous report<sup>13</sup> and our FT-IR measurements. This transient spectrum clearly represents the bleach of the absorption of the C-O stretching vibration of the bound CO molecules. The red absorption tail is probably caused by inhomogeneity of the protein structures. It is uncertain if there are several clearly distinct taxonomic states in CooA, similar to those existing in Mb.<sup>31,32</sup> The main absorption peak though is much stronger than the tail, which suggests that one taxonomic state is predominant. The spectral width of the main peak of the transient spectrum is  $\sim 14 \text{ cm}^{-1}$ , similar to that of Mb-CO ( $12.5 \text{ cm}^{-1}$  measured in this work and  $13 \text{ cm}^{-1}$  from ref 36).

The decay dynamics of the bleach signal at  $1977 \text{ cm}^{-1}$  are shown in Figure 2a. The decay can be well-fitted by a two-exponential decay function having a fast component of  $(56 \pm 7) \text{ ps}$  (55%), a slow component of  $(290 \pm 40) \text{ ps}$  (43%), and a nondecaying component of 2% relative amplitude (fit is not shown). This decay is assigned to the rebinding process of the CO molecule to the heme. Judging from the recombination time, the rebinding is a geminate recombination process. It was shown that binding of CO from solution to the heme of the CooA is a very slow bimolecular process with a rate constant of about  $10 \mu\text{M}^{-1} \text{ s}^{-1}$ .<sup>13</sup> Accordingly, if CO escapes from the heme pocket,

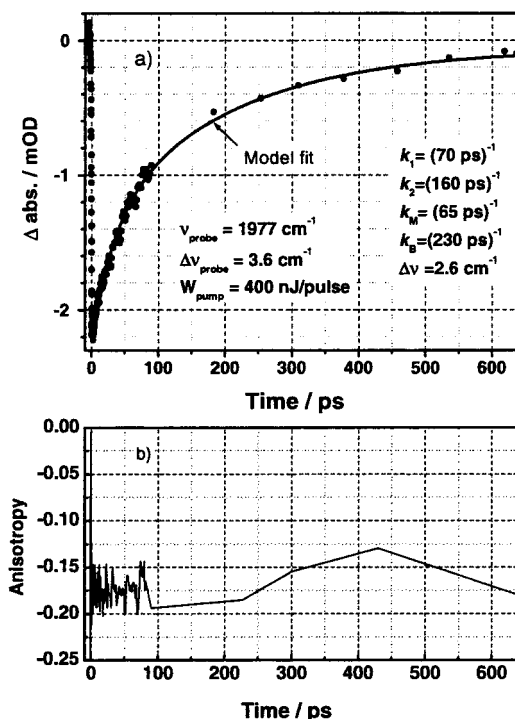


**Figure 2.** (a) Transient bleach signal measured at  $1977 \text{ cm}^{-1}$  with a spectral resolution of  $3.6 \text{ cm}^{-1}$  at perpendicular polarization. The fit curve is presented with parameters shown in the graph. (b) Time-resolved anisotropy.

the rebinding time will be on the order of milliseconds. In CooA, not more than 2% (the nondecaying component amplitude) of photodissociated CO can escape from the heme pocket, which is much smaller than that for Mb (96%)<sup>20</sup> or Hb (>99% in T state and  $\sim 40\%$  in R state).<sup>19</sup> The nonexponential character of the recombination will be discussed below.

**B. Anisotropy of the Bound CO.** The time-resolved anisotropy of the C-O stretching mode is constructed from the parallel and perpendicular polarization components measured separately. No significant change in the anisotropy over time is observed up to several hundreds of picoseconds (Figure 2b). This suggests that the rebound CO quickly takes an orientation similar to the equilibrium one, because there is no change in the anisotropy during the recombination process.

The value of the initial anisotropy is close to  $-0.2$ , the value that corresponds to the perpendicular orientation of two transition moments. Particularly, the initial anisotropy value averaged over several experiments is  $-0.175 \pm 0.003$ . Because about 20% of the hemes are excited, the correction for a finite bleaching<sup>46,47</sup> gives an anisotropy value of  $-0.187 \pm 0.005$ , with the sample treated as an optically thick sample. The transition moment for heme absorption at 400 nm is directed in the porphyrin plane, while the transition moment of the C-O stretch transition is directed along the C-O line. On the basis of the anisotropy value, the angle between the C-O line and the porphyrin plane can be estimated.

In the approximation of a heme as a molecule with linear transition at 400 nm, the angle between the two transition moments can be estimated by eq 1.

$$r(\varphi) = 0.2 (3 \cos^2 \varphi - 1) \quad (1)$$

Here,  $r(\varphi)$  is the initial anisotropy, and  $\varphi$  is the angle between

(46) Hansen, P. A.; Moore, J. N.; Hochstrasser, R. M. *Chem. Phys.* **1989**, 131, 49–62.

(47) Ansari, A.; Szabo, A. *Biophys. J.* **1993**, 64, 838–851.



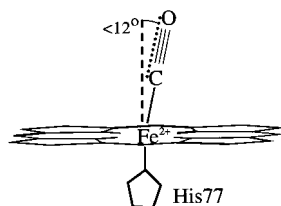


**Figure 3.** Sketch of the CO bound to the CooA protein.

the transition moment at 400 nm and the mid-IR transition of the CO stretching vibration. In this approximation,  $\varphi$  is calculated to be  $82^\circ$ . As an iron porphyrin has a pseudo  $D_{4h}$  symmetry, it behaves as a circular or slightly elliptical absorber. This conclusion is supported by the heme absorption spectrum, which does not show any splitting of the Soret and Q bands. Assuming that the heme is a circular absorber, eq 2 is obtained.

$$r(\varphi) = 0.1 (3 \cos^2 \varphi - 2) \quad (2)$$

The angle  $\varphi$ , which is the angle between the porphyrin plane and the CO vector, is calculated to be  $78 \pm 3^\circ$ .

To get a reference anisotropy value, a sample of horse Mb–CO in  $D_2O$ /glycerol = 1/1 has been measured. The obtained value of  $-0.197 \pm 0.005^{48}$  corresponds to an angle of  $84^\circ$ . This can be considered as the lowest limit for this angle, because no distribution of the bound angles is considered in this model. The anisotropy value obtained is close to the one previously measured,  $-0.192 \pm 0.002$ .<sup>26</sup> The CO vector deviates from the normal to the porphyrin plane in CooA (Figure 3) to a greater extent than in Mb ( $12$  vs  $6^\circ$ ).

A static and dynamic distribution of the binding angles (inhomogeneity) also affects the anisotropy value. Assuming the average binding angle to be  $90^\circ$ , a Gaussian distribution with a width of  $12.5^\circ$  (fwhm) gives the same anisotropy value as observed ( $-0.187$ ). However, no orientational relaxation of bound CO was observed for Mb by mid-IR pump/mid-IR probe experiment,<sup>36</sup> which suggests that dynamic effects are not significant. At the same time, the existence of different conformations with different CO binding angles is possible. In this case, the obtained angle of  $12^\circ$  reflects the distribution width of static inhomogeneity.

**C. Dynamic Spectral Shift.** A small but clear shift of the bleach spectrum to lower frequencies was found during the recombination process (Figures 4 and 5). The spectral shift is distinct in both spectral and kinetic measurements (i.e., decay profiles are different at different wavelengths). The characteristic time for the spectral shift is  $\sim 160$  ps (Figure 4). It is worth mentioning that the contribution of the “red” tail with respect to the main peak in transient spectra remains unchanged over time. So, the spectral shift is not caused by an increased contribution of the structural subset different from the predominant structure. No anisotropy change was observed at any frequency around  $1979 \text{ cm}^{-1}$ .

## Discussion

**A. Reaction Dynamics and Spectral Shift.** The frequency of the CO stretching mode in CooA is about  $35 \text{ cm}^{-1}$  higher than that in horse Mb, giving a smaller binding energy of CO in CooA. The CO frequency in CooA is close to the maximum value observed for different myoglobins.<sup>34</sup> This indicates a low electrostatic potential on the distal side of the heme in CooA (see section H for further discussion). We found that the angle

(48) The measured anisotropy value for the Mb–CO sample was  $-0.184 \pm 0.003$ . Taking into account a finite bleach of the sample (about 25%), the value of  $-0.197 \pm 0.005$  was calculated.

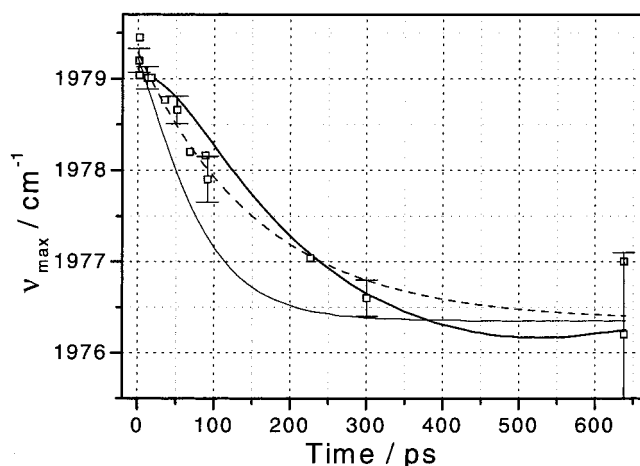


**Figure 4.** Dependence of the peak position of the bleach signal on the delay time. Experimental points (squares) are obtained from the fit of the experimental transient spectra by a Gaussian function. Representative error bars are shown for some points. Thick line shows the best fit according to Scheme 1 with  $k_1 = (70 \text{ ps})^{-1}$ ,  $k_2 = (160 \text{ ps})^{-1}$ ,  $k_M = (65 \text{ ps})^{-1}$ ,  $k_B = (230 \text{ ps})^{-1}$ , and  $\Delta\nu = 2.6 \text{ cm}^{-1}$ . Thin line is the best fit according to the simplified model:  $k_{10} = (55 \text{ ps})^{-1}$  (54%),  $k_{20} = (247 \text{ ps})^{-1}$  (44%), and  $\Delta\nu = 10.2 \text{ cm}^{-1}$ . The dashed line is a single-exponential fit with  $\nu_0 = 1976.4 \text{ cm}^{-1}$ ,  $\Delta\nu = 2.9 \text{ cm}^{-1}$ , and  $\tau = 160 \text{ ps}$ .

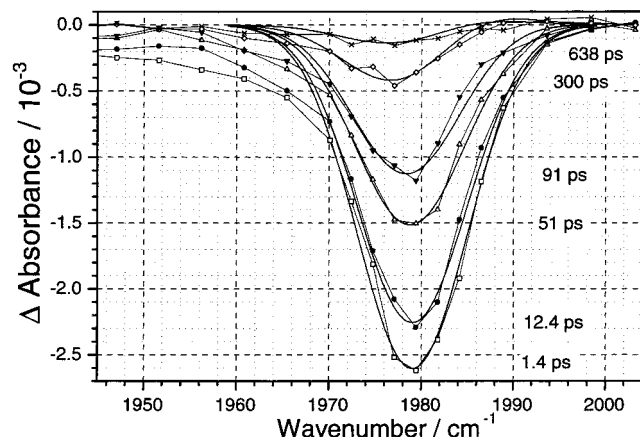


**Figure 5.** Transient spectra (perpendicular polarizations) measured at six time delays: 1.4, 12.4, 51, 91, 300, and 638 ps. The fit curves with the following parameters are shown:  $k_1 = (70 \text{ ps})^{-1}$ ,  $k_2 = (160 \text{ ps})^{-1}$ ,  $k_M = (65 \text{ ps})^{-1}$ ,  $k_B = (230 \text{ ps})^{-1}$ , and  $\Delta\nu = 2.6 \text{ cm}^{-1}$ .

of the C–O axis and the normal to the porphyrin plane is small ( $\leq 12^\circ$ ), though it is larger than those for Mb ( $< 7^\circ$ ) and Hb ( $\sim 10^\circ$ ). These observations can be accounted for by a tighter protein structure on the distal side and/or the influence of the low polarity around the attached CO. A decrease in the back electron donation from the Fe atom at a more distorted CO geometry could be another reason for the increase in the CO frequency.

Upon photoexcitation of the heme, CO dissociates with essentially unit probability. The dissociated CO is “docked” somewhere near the heme (Scheme 1, reaction 1) on a much faster time scale than for the other processes. Recombination dynamics show nonexponential behavior, which formally indicates that there are at least two states from which the recombination can occur. Three general possibilities are considered for these states. It could be that different protein conformations exist in the sample before photoexcitation or different docking sites of dissociated CO exist. It is also reasonable that the conformational change of the protein, started

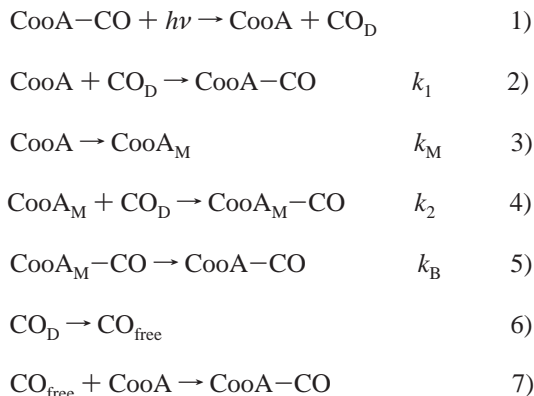
by CO dissociation, changes the recombination probability. In the latter case, a creation of the modified protein conformation (denoted as CooA<sub>M</sub>) slows down the recombination rate.

Another observation to be taken into account in the model is the shift over time in the transient spectrum. The characteristic time of the spectral shift is close to the average recombination time (160 ps), calculated as a weighted average of the two decay components. As the observable in this experiment is the transient spectrum of the bound CO, the frequency of the bound CO has to change over time after photoexcitation. We suggest that the CO frequency is different in the equilibrium CooA–CO protein conformation and in the modified protein conformation (CooA<sub>M</sub>), with the latter being higher, judging from the direction of the observed spectral shift. The possibility of the influence of one monomer upon another in the CooA homodimer is considered in section F.

To establish the importance of different states for the CO recombination process, we constructed several working schemes with different major states involved in the recombination reaction and spectral shift.

**B. Recombination Rate Correlated with the Protein Conformation.** In Scheme 1, we assume that there is only one equilibrium protein conformation for the CO bound state (denoted as CooA) and that there is only one docking site for the dissociated CO (CO<sub>D</sub>) (reaction 1). CO dissociation induces the protein conformational change (reaction 3). The formation of a different protein conformation (CooA<sub>M</sub>) has two effects. The recombination rate (reaction 4) is slower ( $k_2 < k_1$ ), and the CO stretching frequency is higher, when the protein is in the CooA<sub>M</sub> conformation.

Scheme 1



So, reaction 2 is associated with the fast component in terms of recombination dynamics while reaction 4 describes the slow component. Reaction 5 stands for the recovery of the protein conformation back to the equilibrium CO–bound conformation. The last two reactions describe a release of the dissociated CO from the heme pocket and a bimolecular rebinding reaction. We found that the quantum yield of CO release from the protein pocket (reaction 6) is quite small and is estimated to be less than 2% (Figure 2a). The last reaction was shown to be very slow<sup>13</sup> and can be considered to be infinitely slow on a subnanosecond time scale. Because of a very small CO escape quantum yield and slow nongeminate recombination, these two reactions were not included in the modeling.

Differential equations corresponding to reactions 2–5 were solved analytically under initial conditions where only the concentration of the CooA state is nonzero at  $t = 0$ . The spectral shift, observed in this work, is associated with the difference in frequencies of the bound CO between the two protein

conformations, CooA and CooA<sub>M</sub>. The shape of the transient spectra has a dip around 1990 cm<sup>-1</sup>, which suggests that the rebound CO (CooA<sub>M</sub>) has a higher frequency than CO before excitation. The spectra of the bound CO at these two states are simulated by two Gaussian functions with the same width obtained from the fit of the transient spectra at early time delays (<10ps). The central frequency of the CO vibration in the equilibrium CooA–CO conformation obtained from the fit is 1979.2 cm<sup>-1</sup>. The central frequency of the CO stretching vibration in the CooA<sub>M</sub>–CO conformation as well as the rate constants of reactions 2–5 were treated as fit parameters.

According to the model (reactions 2–5), spectra at different delay times (Spec( $\omega, t$ )) are fitted by eq 3, in which the transient absorption spectrum at time delay  $t$  is the difference between spectrum  $x(t)*\text{Sp}_x(\omega) + y(t)*\text{Sp}_y(\omega)$  and the spectrum of the nonexcited protein,  $\text{Sp}_x(\omega)$ .

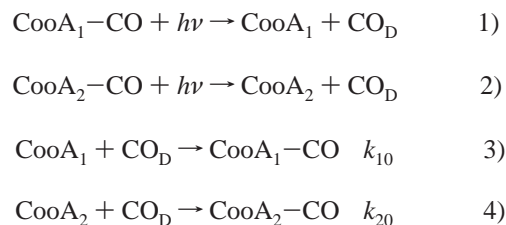
$$\text{Spec}(\omega, t) = (x(t) - 1)\text{Sp}_x(\omega) + y(t)\text{Sp}_y(\omega) \quad (3)$$

Here,  $x(t)$  and  $y(t)$  are the relative ratios of the concentrations of CooA–CO and CooA<sub>M</sub>–CO states to the total photolyzed molecules, respectively, and  $\text{Sp}_x(\omega)$  and  $\text{Sp}_y(\omega)$  are their spectra. By fitting the spectra at different delay times, a good agreement was obtained (Figures 2a, 4, and 5). The frequency of the rebound CO (CooA<sub>M</sub>–CO) is found to be  $\sim 2.6$  cm<sup>-1</sup> higher than that for the equilibrium CooA–CO state. The peak positions for the CO frequencies of the equilibrium (CooA–CO) and transient (CooA<sub>M</sub>–CO) states are 1979.2 and 1981.8 cm<sup>-1</sup>, respectively. The CO recombination rate constants for the two states differ by a factor of more than two, with  $k_1 = (70 \text{ ps})^{-1}$  and  $k_2 = (160 \text{ ps})^{-1}$ . The rate of reaction 3 is about the same as  $k_1$ ;  $k_M = (65 \text{ ps})^{-1}$ . The value of  $k_B$  is estimated to be about  $(230 \pm 70)^{-1} \text{ ps}^{-1}$ .

An impressively good fit of the model to both the spectral change and recombination reaction kinetics supports the idea that the recombination rate constant could be altered by the transient protein conformation change. An alternative way of explaining the nonexponential recombination rate is to consider multiple arrangements of the reactants.

**C. Multiple Conformations.** Here, we assume that there are two equilibrium protein conformations of the CO bound state (CooA<sub>1</sub> and CooA<sub>2</sub>) and only one docking site for the dissociated CO (CO<sub>D</sub>). To explain nonexponential recombination dynamics, the recombination rates are different in the two protein conformations (reactions 3 and 4). The CO stretching frequencies are also different in the two protein conformations CooA<sub>1</sub> and CooA<sub>2</sub>.

Scheme 2

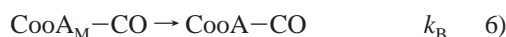
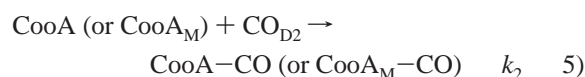
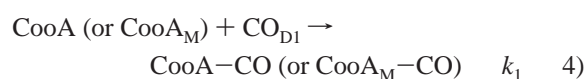


This model, though even simpler than the previous one, cannot explain the whole set of data. The spectral shift predicted by this model proceeds on the same time scale as the fast recombination rate. However, in the experiment, the spectral shift ( $\sim 160$  ps) is more than twice as slow as the fast component of the recombination kinetics ( $\sim 70$  ps). Though the recombination kinetics can be fitted well (not shown), the spectral shift

cannot be fitted well if taken together with recombination decay (thin line in Figure 4).

**D. Spectral Shift Independent of the Recombination Reaction.** In both models (Schemes 1 and 2), the recombination reaction and spectral shift are closely related, because the same states are responsible for both effects. Inclusion of multiple docking sites for CO ( $\text{CO}_{\text{D1}}$  and  $\text{CO}_{\text{D2}}$ ) allows one to separate two processes; the recombination reaction can be nonexponential because of the existence of different docking sites, while the spectral shift is determined by protein conformation dynamics and is independent of the recombination reaction.

Scheme 3



One can assume that the protein conformation change (reaction 3) does not affect the recombination rate constants between heme and CO ( $k_1$  and  $k_2$ ) or at least that this dependence is not very significant. The two exponential times ( $\tau_1 = 56$  ps (55%) and  $\tau_2 = 290$  ps (43%)) of the recombination kinetics are presented by the two reaction rates of  $\text{CO}_{\text{D1}}$  and  $\text{CO}_{\text{D2}}$  ( $k_1 = 1/\tau_1$  and  $k_2 = 1/\tau_2$ ). The dynamic peak shift in this model is independent of the recombination rate constants  $k_1$  and  $k_2$ . The peak shift dynamics are generally nonexponential, but rather S-like, similar to that in Scheme 1. In the limiting case of  $k_{\text{M}} \gg k_{\text{B}}$ , the spectral shift function is close to exponential, in which  $k_{\text{B}}^{-1} = 160$  ps. The parameters  $k_{\text{M}}$ ,  $k_{\text{B}}$ , and the central frequency of the  $\text{CooA}_{\text{M}}\text{-CO}$  spectrum cannot be uniquely determined in this model from the available data. For example, the same parameters (except  $k_1$  and  $k_2$ ) obtained in Scheme 1 give a similarly good fit. Another set of values also gives a good fit:  $k_{\text{M}} = (40 \text{ ps})^{-1}$ ,  $k_{\text{B}} = (270 \text{ ps})^{-1}$ , and  $\nu(\text{CooA}_{\text{M}}\text{-CO}) = 1981.2 \text{ cm}^{-1}$ . A good fit can be obtained when the  $k_{\text{M}}$  rate constant is in the range  $(20\text{--}70 \text{ ps})^{-1}$ , with the respective change of  $\nu(\text{CooA}_{\text{M}}\text{-CO})$ . Only recombination rates,  $k_1$  and  $k_2$ , can be determined accurately in the framework of this model on the basis of the data available.

It would be worth mentioning two relatively close rate constants, one observed in the present paper and one in ref 14. The visible pump-probe study on CooA has shown a 173 ps component in the Soret band region in the reduced form of CooA that does not have CO.<sup>14</sup> Although this time constant seems to be rather close to the characteristic time (160 ps) of the spectral shift, the decay dynamics come from two distinctly different samples, that is, CooA protein without CO in the visible spectra and with CO in the IR spectra. In fact, the dynamics with CO observed in the visible region are completely different (78 and 400 ps) from those without CO (6.5 and 173 ps).<sup>14</sup>

**E. Heme Heating Effect.** Another effect, which might cause the spectral shift, is heating of the heme. The temporal temperature elevation of the protein caused by photoexcitation

of the heme is quite large ( $\sim 600$  K). The quantum yield of dissociation in Mb and Hb was reported to be close to 100%.<sup>18</sup> Because the phenomenon under observation in this work is the absorbance change of the bound CO, there should be no signal associated with vibrationally hot hemes until CO recombines. At the same time, it was shown that cooling of the heme is quite fast.<sup>22,23,31,49,50</sup> In a protein, the rate of the cooling is about  $(10 \text{ ps})^{-1}$ . Even for ligated heme in solution where heat transfer is much slower than in a protein, the relaxation time of a CO vibration is on the order of 40 ps.<sup>22,23</sup> The characteristic time of the spectral shift (160 ps, Figure 4) is much longer than the expected cooling time. This allows us to conclude that the protein conformational change rather than local heme temperature is the origin of the spectral shift.

**F. Allosteric Influence of One Heme on Another.** The dynamic spectral shift can be related to the dimeric structure of the CooA protein. The CooA protein in the presence and absence of CO was found to be a homodimer.<sup>8,9</sup> If a heme in only one part of the dimer is excited, its CO molecule dissociates, and the protein conformation presumably starts to change to an inactive one. What happens to the other heme in the dimer? It seems possible that it will be affected by the conformation change in its counterpart in the dimer. One may expect a decrease in the CO binding energy in the unexcited heme of the dimer, facilitating the switch of the whole protein from the active conformation (with both CO molecules attached) to an inactive one (without any ligated CO). A decrease in the binding strength is concomitant with an increase in the CO stretching frequency. The latter will cause a spectral shift in the bleach spectrum to a lower frequency, as observed. Thus, the allosteric influence in the dimer may cause the observed spectral shift. This effect can be treated in the same way as the model presented in Scheme 3. Reaction 3 in this case should be rewritten as follows.



Here,  $\text{CooA}'\text{-CO}$  stands for the part of the dimer with an unexcited heme, while the heme in the adjacent part of the dimer was excited. Now the CO frequency changes in the heme, which was not excited, and the change happens as a result of the influence exerted by the counter-heme in the dimer. With the only difference being in the assignment of reaction 3, Scheme 3 can be used. The  $k_{\text{M}}$  rate constant, which is in the range  $(20\text{--}70 \text{ ps})^{-1}$ , is treated here as the allosteric influence of one heme on another in the CooA dimer. Even taking into account that in the inactive conformation the Pro2 terminal group of one subunit is the axial ligand of the heme surrounded by another subunit in the dimer, the time of 20–70 ps seems to be too fast for such an assignment.

**G. Conformational Change of the Protein.** While we concluded that the observed spectral shift is associated with dynamic protein conformational change, triggered by CO dissociation, it is interesting to specify in more detail those conformational changes. Any protein conformational change is a complicated process, all of which proceed at a variety of characteristic times. Because the CO frequency shift observed in this work is most sensitive to the spatial arrangement of the heme pocket on the distal side, the observed rate of about  $(160 \text{ ps})^{-1}$  seems to be attributable to the conformation change in the CooA protein on the distal side of the heme.

A visible pump-probe experiment in the Soret band region carried out in our laboratory has shown that the decay dynamics of the five-coordinate heme after the CO-photolysis are in good agreement with the recombination dynamics of the bleaching



signal of the ligated CO band in this study.<sup>14</sup> It is thus likely that the original distal ligand in the reduced CO-free CooA, Pro2, or any other ligand does not ligate the heme before CO is rebound. However, it is still possible that the conformational change in a distal ligand disturbs CO from ligating the heme, which causes the observed two-exponential recombination kinetics. If so, inferred from  $k_M$ , the time for ligation of another ligand is on the order of tens of picoseconds.

An iron motion is another possible cause of conformation change. There are theoretical predictions for Mb that show conformation changes caused by an iron motion out of the heme plane.<sup>1</sup> The recombination rate might also decrease as the iron atom moves out of the heme plane toward the proximal ligand. However, iron out-of-plane motion itself is supposed to be faster than 10 ps. The time-resolved Raman spectroscopy of the iron–histidine stretching mode in Mb suggests that a time of  $\sim 10$  ps is necessary for iron out-of-plane displacement.<sup>35</sup> At the same time, slower dynamics with a time of  $\sim 100$  ps were observed in the same work. However, changes in the amide-I band of Mb after CO dissociation were observed with a characteristic time of 8 ps,<sup>51</sup> suggesting that some conformational changes in Mb may happen without much delay.

The geminate recombination reaction of CO in CooA is significantly faster than that for Mb or Hb, where the rebinding time is on the order of several microseconds.<sup>20</sup> This suggests that the CO docking place is probably located close to an iron atom and does not substantially retard recombination. The tight structure of the heme pocket on the distal side of the heme in CooA protein could be one reason for the fast CO recombination.

In any case, there are conformational changes in the protein pocket, which cause an upshift of the CO frequency. Though the geometry of the bound CO can be affected by steric constraints, it is generally accepted that the frequency of the bound CO is mostly affected by electrostatic interactions rather than by steric hindrance.<sup>33,34</sup> The value of the frequency, observed for CO in CooA ( $1979.2\text{ cm}^{-1}$ ), is rather high, indicating that there are noncharged or negatively charged groups surrounding the bound CO molecule. The observed frequency shift can be accounted for by the approach of negatively charged groups caused by the conformational changes.

**H. Geometry of the Bound CO.** The CO anisotropy measured in this work revealed that CO is bound to the heme when the angle between the heme plane and the CO bond is  $\geq 78^\circ$ . The recent EXAFS analysis of the CO-bound CooA has, however, indicated that the Fe–CO complex in the CO-bound CooA is linear at an Fe–C–O angle of  $180^\circ$ .<sup>52</sup> The measurements of the CO anisotropy were carried out with the sample in solution at room temperature, while EXAFS measurements were made in a frozen solid sample at liquid nitrogen temper-

ature. Though the experimental conditions of these two experiments were not the same, there is a geometry which can satisfy both results (Figure 3). To achieve this, the Fe–C bond should be tilted with respect to the normal to the heme plane. This geometry seems not unreasonable, because about a  $4.7^\circ$  tilt of the Fe–C bond from the normal has been observed for Mb from its crystal structure.<sup>29</sup>

The geometry of the bound CO ( $\alpha \leq 12^\circ$ ) can be influenced by the existence of another distal ligand in the vicinity, which ligates the heme in the absence of CO. This ligand can exert spatial or electrostatic constraints on the bound CO and force it to be bent out of the normal to the porphyrin plane. No change in the anisotropy was observed during the recombination process (Figure 2b), indicating that the rebound CO quickly takes the same orientation as that in the equilibrium CooA–CO state. In other words, the bound angles of CO are similar for both protein conformations (CooA–CO and CooA<sub>M</sub>–CO).

Recently, the crystal structure of the reduced CooA has been reported.<sup>16</sup> Though the structure of the distal side of the heme pocket will probably be different for the reduced and CO-bound forms (and only the structure of the reduced form has been reported), it is interesting to analyze which amino acid residue can cause the blue shift of the CO stretching vibration. On the basis of the reported structure of the reduced CooA, there are no negatively charged residues in the distal side of the heme pocket. The only closely located negatively charged group is Pro2, which is dissociated from the heme iron upon CO binding. The imino nitrogen of Pro2 is thought to be deprotonated when it is coordinated to the ferrous heme. The negatively charged Pro2 will be located around the bound CO after dissociation from the heme upon CO binding, which may be the source of the negative charge.

In conclusion, the CooA protein, which is a transcriptional regulator allosterically controlled by CO binding, was studied by time-resolved visible-pump mid-IR-probe spectroscopy. A large conformation change is expected for this protein upon CO dissociation, which switches the protein from the active conformation toward the inactive one. The spectral shift of the bound CO stretching mode was detected at a time constant of about hundred picoseconds, thus providing an estimation for the initial step of the biologically relevant protein conformation change. The geometry of the bound CO in CooA was determined by means of time-resolved mid-IR anisotropy measurements.

**Acknowledgment.** Suggestions by Professors Gilbert Walker and Hiromi Okamoto for construction of the IR spectrometer are greatly acknowledged. T. Zhang thanks the Inoue Science Foundation and the Japan Society for Promotion of Science for the postdoctoral fellowship. This work is supported in part by the grant-in-aid program for scientific research (11554028, 12680631, 12147203, and P00125) of the Ministry of Education, Science, Sports, and Culture of Japan.

JA011023W

(49) Hill, J. R.; Ziegler, C. J.; Suslick, K. S.; Dlott, D. D.; Rella, C. W.; Fayer, M. D. *J. Phys. Chem.* **1996**, *100*, 18023–18032.

(50) Peterson, K. A.; Rella, C. W.; Engholm, J. R.; Schwettman, H. A. *J. Phys. Chem. B* **1999**, *103*, 557–561.

(51) Causgrove, T. P.; Dyer, R. B. *J. Phys. Chem.* **1996**, *100*, 3273–3277.

(52) Nakajima, H.; Honma, Y.; Tawara, T.; Kato, T.; Park, S. Y.; Miyatake, H.; Shiro, Y.; Aono, S. *J. Biol. Chem.* **2001**, *276*, 7055–7061.